Electronic potential of a chemisorption interface

Jin Zhao,[1] Niko Pontius,[1,2] Aimo Winkelmann,[1,3] Vahit Sametoglu,[1] Atsushi Kubo,[1,4] Andrei G. Borisov,[5] Daniel Sánchez-Portal,[6,7] V. M. Silkin,[6,7] Eugene V. Chulkov,[6,7] Pedro M. Echenique,[6,7] and Hrvoje Petek[1,6,*]

[1]*Department of Physics and Astronomy, University of Pittsburgh, Pittsburgh, Pennsylvania 15260, USA*

[2]*BESSY mbH, Albert-Einstein-Str. 15, 12489 Berlin, Germany*

[3]*Max-Planck-Institut für Mikrostrukturphysik, Weinberg 2, D-06120 Halle, Germany*

[4]*PRESTO, Japan Science and Technology Agency, 4-1-8 Honcho Kawaguchi, Saitama, Japan*

[5]*CNRS, Laboratoire des Collisions Atomiques et Moléculaires, UMR 8625, Université Paris-Sud, Orsay, F-91405, France*

[6]*Donostia International Physics Center (DIPC), Paseo Manuel de Lardizabal 4, San Sebastián 20018, Spain*

[7]*Centro de Física de Materiales CSIC-UPV/EHU and Departamento de Física de Materiales, Facultad de Química, UPV/EHU, Aptd. 1072, San Sebastián E-20080, Spain*

(Received 19 February 2008; revised manuscript received 5 May 2008; published 13 August 2008)

Chemisorption of atoms and molecules controls many interfacial phenomena such as charge transport and catalysis. The question of how the intrinsic properties of the interacting materials define the electronic structure of their interface remains one of the most important, yet intractable problems in surface physics. Through two-photon photoemission spectroscopy we determine a common binding energy of ~1.8–2.0 eV with respect to the vacuum for the unoccupied resonance of the *ns* valence electron of alkali atoms (Li-Cs) chemisorbed at low coverage (less than 0.1 monolayer) on noble metal [Cu(111) and Ag(111)] surfaces. We present a theoretical model based on the semiempirical potentials of the adsorbates and the substrates, their principal mode of interaction through the Coulomb interaction, and the *ab initio* adsorption structures. Our analysis reveals that atomic size and ionization potential independent interfacial electronic structure is a consequence of the Coulomb interaction among the *ns* electron, the alkali-atom ionic core, and the induced image charge in the substrate. We expect the same interactions to define the effective electronic potentials for a broad range of molecule/metal interfaces.

DOI: 10.1103/PhysRevB.78.085419 PACS number(s): 73.20.−r

I. INTRODUCTION

Just as the Mott-Schottky model[1,2] for the band alignment at semiconductor interfaces paved the way for the semiconductor-transistor-based electronic industry, the emerging application of molecule-based electronics requires the knowledge of how the properties of the free adsorbates and clean surfaces define their interfacial potential on the atomic scale.[3–6] Although first-principles theoretical methods can predict accurately the geometrical structures of adsorbates on metals, to describe the electronic structure of such interfaces remains a formidable challenge of fundamental and practical interest.[7–15] Having a simple method to predict the electronic properties of an interface from those of the unperturbed surface and free adsorbate and their primary mode of interaction would greatly advance our ability to design novel molecule-based electronic devices.[3]

Alkali atoms, with a single *ns* valence electron, constitute one of the simplest models for theories of chemisorption on metal surfaces.[16–23] Despite being one of the earliest chemisorption systems to be studied, describing the chemisorption state of alkali atoms on metals has presented both experimental and theoretical difficulties. Although one expects substantial charge transfer of the valence *ns* electron of alkali atom to the substrate, the occupied density of states (DOS) of the chemisorbed system, which corresponds to a delocalized *ns* valence electron of alkali atom in the conduction band of the substrate, is spectroscopically silent.[24] In part because it is difficult to characterize spectroscopically, the degree to which the chemisorption bond can be described as ionic or covalent has been controversial.[25–27] The experimental understanding of the electronic structure of alkali atoms has been greatly expanded by spectroscopy of the unoccupied DOS of alkali-atom-covered metal surfaces,[28] particularly by the two-photon photoemission (2PP) technique.[8–10,29–35] Until now, however, there have been no systematic studies of the unoccupied electronic structure of alkali-atom-covered surfaces as a function of the alkali-atom period, coverage, and the metal substrate. Here we present a joint 2PP experimental and theoretical study of alkali-atom chemisorption on noble metals. To rationalize the observed material and coverage trends, we develop a simple model, based on the ideas already elaborated in literature beginning with the pioneering work of Langmuir,[17] that describes accurately the electronic structure of the alkali atom/noble metal interface and can be generalized to other chemisorption systems for which the valence charge is well localized in electronic orbitals of the atomic or molecular adsorbate.

II. EXPERIMENT

The clean Cu(111) and Ag(111) surfaces were prepared by standard surface science methods under ultrahigh-vacuum conditions. Continuous effusive beams from commercial getter sources were used to deposit alkali atoms onto the clean surfaces. Great care was taken to align each beam in order to obtain uniform alkali-atom coverage and thereby avoid surface-field gradients. Two-photon photoemission was excited with 10 fs pulses from the second harmonic of a self-made, negative dispersion mirror, Ti:sapphire laser oscillator,

(3.1 eV photon energy) as described previously.[36–38] The photoemission yield normal to the surface was recorded with a hemispherical energy analyzer equipped with a seven-channel channeltron detector array. 2PP spectra [Fig. 1(a)] were acquired sequentially during the continuous alkali-atom deposition onto Cu(111) and Ag(111) surfaces at 300 K. The deposition was started by opening a shutter after taking a 2PP spectrum of the clean surface [shaded in Fig. 1(a)]. Decreasing of the work function Φ with increasing alkali-atom coverage, which can be seen as the decreasing low-energy cutoff in the 2PP spectra of Fig. 1(a) for Cs/Cu(111), caused by the onset of intense one-photon photoemission for $\Phi < 3.4$ eV. The space-charge effects caused by one-photon photoemission interfered with the acquisition of 2PP spectra, thereby limiting the maximum alkali-atom coverage that could be studied to less than 0.1 monolayer (ML). The work function change could be compared to the previously reported measurements in order to estimate the alkali-atom coverage.[30,39]

III. RESULTS AND ANALYSIS

Experimental 2PP spectra in Fig. 1(a) provide a window on how the electronic structure of the alkali atom (Li through Cs)/noble metal interface depends on the fundamental properties of the adsorbates, such as their sizes and the ionization potentials, and how it evolves as the function of the adsorbate coverage. As the alkali-atom coverage is progressively increased, the 2PP spectra reflect gradual chemisorption-induced changes, both in the decrease of the work function, indicated by $\Delta\Phi$ in Fig. 1(a), and in the appearance of distinct resonances.[8,10]

Figure 1(b) shows the possible excitation pathways for the 2PP process involving the charge-transfer excitation from the initial states of the substrate (bulk and surface) to the intermediate unoccupied *ns* resonance of alkali atoms (6s in the case of Cs). Because of its wave function and repulsive interaction with the substrate, we refer to this unoccupied state as the antibonding resonance [AR; red line in Fig. 1(b)]. Because the unoccupied orbital is localized on an alkali atom, the optical transition need not conserve the parallel momentum. Therefore, the excitation process integrates over all momentum states (parallel and perpendicular) that conserve energy, and have wave function overlap between the initial and intermediate states in the 2PP process. For example, the excitation can occur from the partially occupied Shockley surface state [SS; green line in Fig. 1(b)], which exists within the *L*-projected band gaps of (111) surfaces of noble metals, as long as the maximum energy separation between AR and SS does not fall below the photon energy of 3.1 eV. The excitation to AR can also occur from the lower *sp* band (L_{sp}) of the substrate for all initial states that conserve energy. To complete the 2PP process, the electron transiently occupying AR has to be excited above the vacuum level [E_{vac}; blue line in Fig. 1(b)] by absorbing another photon. The final states in the two-photon transition can either be the upper *sp* band (U_{sp}) of the substrate, from which the electron can escape into the vacuum, or a free-electron inverse low-energy electron diffraction (LEED) state.[40] By recording a 2PP spectrum, one obtains information on the joint density of initial and intermediate states that mediate the 2PP process.[38,41] Further details of 2PP spectroscopy of alkali-atom-covered copper surfaces have been reviewed in Refs. 10, 34, and 35.

As can be seen in the spectra of Fig. 1(a) and as described in the excitation scheme of Fig. 1(b), the 2PP spectra also give information on the work function reduction $\Delta\Phi$. Transfer of the *ns* valence electron from an alkali atom to a metal substrate at the chemisorption distance R_{ads} creates a surface dipole of strength $\mu = 2R_{\mathrm{ads}}$ (atomic units are used unless otherwise specified). The development of this surface dipole field is manifested in the 2PP spectra of Cs/Cu(111) in the dramatic decrease in Φ by an amount given by $\Delta\Phi = 2\pi\sigma\mu$, which is proportional to the surface alkali-atom density σ. Because R_{ads} depends on the size of alkali atoms, achieving the comparable $\Delta\Phi$ as for Cs requires proportionally higher coverage for the smaller alkali atoms. In addition to changing the work function, the dipole field also lowers the energies of AR, and to a smaller extent, that of SS. This coverage-dependent tuning of the surface electronic structure is responsible for the changes in the intensity and energy of AR that can be seen in Fig. 1(a).

Resonance peaks in the 2PP spectra provide more detailed information on the σ-dependent interfacial electronic structure. For the clean Cu(111) surface, the only spectroscopic feature in 2PP spectra with 3.1 eV light, indicated by "SS" and the red arrows in Fig. 1(a) for each alkali atom, is the dispersive SS with a band minimum at −0.4 eV below the Fermi level (E_F), which is observed through a nonresonant two-photon excitation process. In the low alkali-atom coverage limit, a new peak, which is indicated by "AR" and the blue arrows in Fig. 1(a), appears in 2PP spectra at an energy above the SS peak. This new feature is the nondispersive AR, which, notably, has nearly the same energy of ~3 eV above E_F for Li through Cs on Cu(111). The 2PP intensity rises with σ, where the SS and AR peaks overlap both through the gain in the density of surface absorbers and the tuning of the AR ← SS transition into resonance with the excitation laser at $k_{\parallel} = 0$. The 2PP intensity reaches a maximum when the AR ← SS transition becomes resonant with the laser, which occurs for the AR energy of 2.50–2.53 eV. When the AR ← SS transition energy drops below 3.1 eV for all $k_{\parallel}$, the excitation from SS no longer can participate in a resonant process, and therefore, the AR intensity begins to decrease. Nevertheless, AR can still be populated by photoinduced charge-transfer excitation from the L_{sp} band of copper. The *d* bands of copper, seen as an additional peak at the initial state of −2.2 eV,[42] are too deep to serve as the initial states for the excitation of AR in a 2PP process with 3.1 eV light.

The 2PP spectra in Fig. 1(a) for the chemisorption of different members of the alkali-atom group show remarkable similarity: in the limit of $\sigma \to 0$, not only does the AR peak appear at essentially the same energy for Li through Cs, but with increasing σ, it is also stabilized with the nearly identical $(\Delta\Phi)^{3/2}$ dependence [Fig. 2(a)].[43] Determining the actual AR energy for the near-resonant AR ← SS excitation on Cu(111) is difficult because a simple deconvolution of lineshapes is not feasible. This is because AR is populated from both SS and the bulk *sp* band at different $k_{\parallel}$, and furthermore,

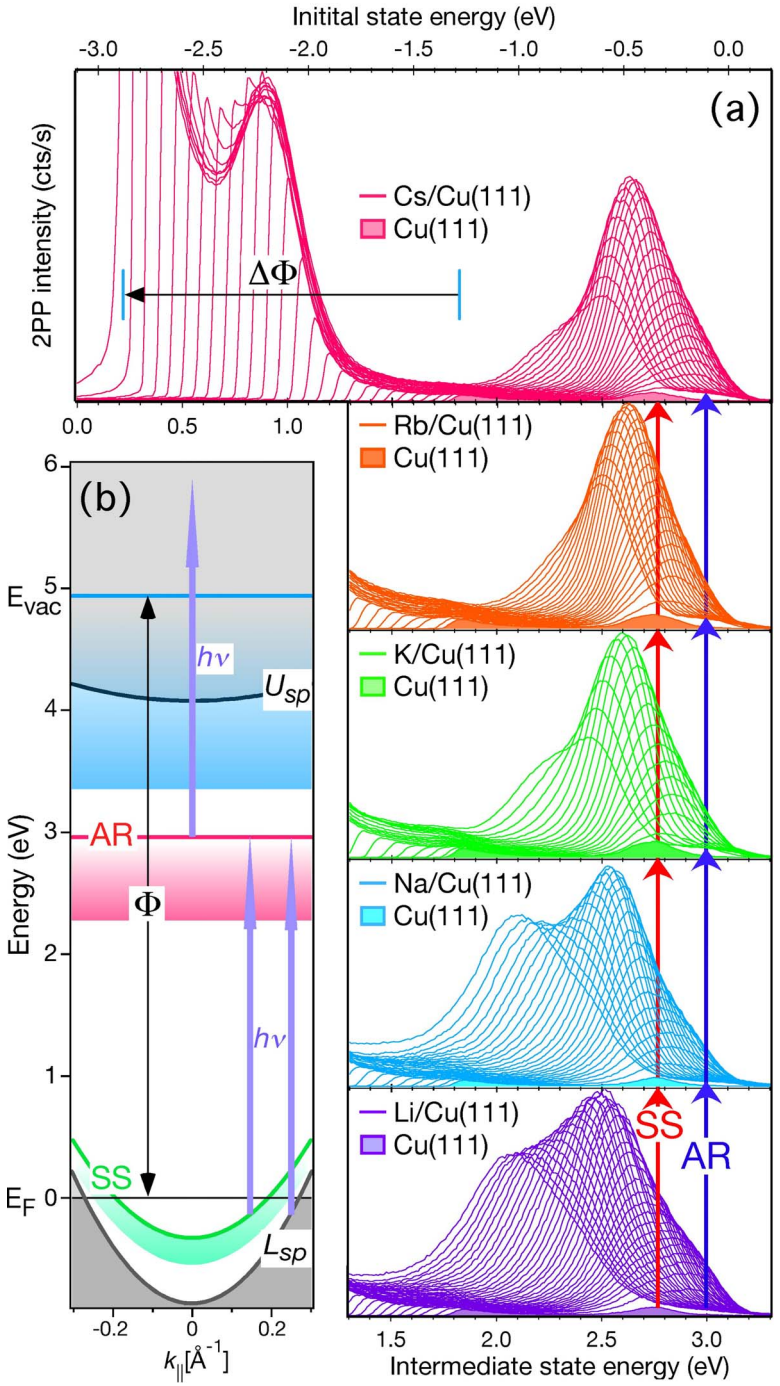

FIG. 1. (Color online) (a) 2PP spectra for Li through Cs on Cu(111) during continuous alkali-atom deposition up to ~0.1 monolayer coverage, plotted against the initial (top) and intermediate (bottom) state energies. The Shockley surface state (SS), marked by "SS" and the red arrows, is the main feature in 2PP spectra of the clean Cu(111) surface (shaded). The antibonding resonance (AR), marked by "AR" and the blue arrows, appears ~2.97 eV above E_F in the zero coverage limit. During the continuous deposition, the formation of a surface dipole field with increasing alkali-atom coverage progressively stabilizes AR, SS, and Φ, causing them to appear at lower energies. The changes in the 2PP intensity reflect the increase in the density alkali-atom absorbers and the tuning of the resonant excitation from the surface and bulk bands of the substrate to AR. ΔΦ indicates the decrease in the work function (low-energy edge of 2PP spectra) with the alkali-atom coverage. (b) The surface-projected band structure as a function of electron momentum parallel to the surface ($k_{\|}$) indicates the possible two-photon excitation pathways involving the AR intermediate state. A projected band gap exists between the lower (L_{sp}) and the upper *sp* bands (U_{sp}). The three-dimensional (3D) bulk L_{sp} and U_{sp} bands disperse along the Γ-*L* line (perpendicular momentum; not shown) within the gray regions below and above the *L*-projected band gap of Cu(111). The green, red, and blue lines (also indicated respectively by "SS," "AR," and "E_{vac}") give the energy of the SS, AR, and E_{vac}, respectively, in the zero coverage limit; the corresponding colored surfaces below the lines indicate the range of their tuning with the alkali-atom coverage. The vertical arrows show possible resonant transitions from SS and L_{sp} to AR at different $k_{\|}$. The final step in the 2PP process is observed for emission normal to the sample surface.

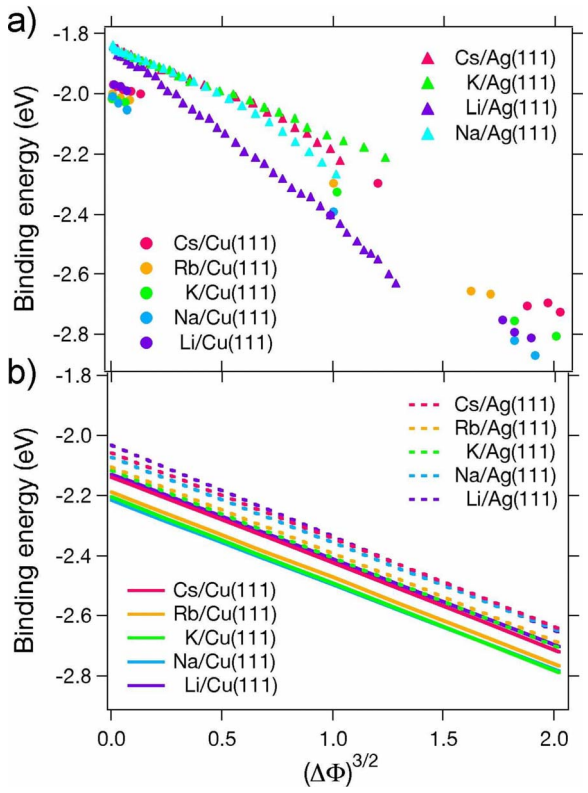

FIG. 2. (Color online) (a) The AR binding energy for different alkali-atom coverages is plotted against $\Delta(\Phi)^{3/2}$ for the Cu(111) and Ag(111) surfaces. For Cu(111), the AR energy is given only at or far from the AR$\leftarrow$SS resonance. The deviation of the AR shift for Li/Ag(111), and to lesser extent Na/Ag(111), from the common $\Delta(\Phi)^{3/2}$ trend of the larger alkalis reflects the diffusion of small alkalis into the Ag(111) substrate (Refs. 7 and 16) (b) The calculated stabilization of the AR binding energy for Cu(111) and Ag(111) by the surface dipole field.

the lineshape is distorted by the alkali-atom desorptive motion.[9,35,44] For this reason, the AR position was estimated either far from resonance, or at the resonance maximum, where the deconvolution was not necessary. We also measured the 2PP spectra of Li, Na, K, and Cs on Ag(111) (not shown). In the case of Ag(111), the AR$\leftarrow$SS resonance energy is always less than the photon energy, which excludes resonant transitions from SS from participating in the 2PP process, and therefore, makes the AR peak-energy determination unambiguous. The AR peak position for Li, and to a smaller extent Na, on Ag(111) deviates from the trends for larger alkali atoms. For Li and Na on Ag(111), after the alkali-atom deposition had been stopped, the AR gradually moved to higher energy and decreased in intensity, suggesting the loss of alkali atoms from the surface. We judge this to be a result of alloy formation, where small alkali atoms diffuse from the surface into the Ag(111) substrate.[7,16] For the larger alkali atoms on Ag(111) and all alkali atoms on Cu(111), the spectra were stable. By measuring the AR binding energy on Ag(111), we confirmed that its independence of the alkali-atom period is not fortuitous. Nevertheless, the common asymptotic ($\sigma \rightarrow 0$) binding energy of AR with respect to the vacuum level, E_{vac}, is $\sim$0.15 eV smaller for Ag(111) than for Cu(111), as shown in Fig. 2(a).

Although alkali atoms show a clear periodic trend of decreasing ionization potential with increasing size, their periodic differences as chemisorbates on noble metal surfaces appear mainly in the AR linewidths, but not in the AR binding energy. Small alkali atoms (Li and Na) chemisorb closer to the surface, where the faster rate of elastic energy-conserving electron transfer into the empty states of the conduction band of the substrate leads to a broader AR linewidth.[10–12] Nevertheless, the AR widths are narrow ($<$200 meV) because the projected band gap between the lower and the upper *sp* bands on (111) surfaces of the noble metals [Fig. 1(b)] restricts the phase space for the decay through the elastic and inelastic electron-decay channels.[8–12]

IV. DISCUSSION

The period-independent energy of the *ns* resonance of alkali atoms and its characteristic stabilization with σ for the Cu(111) and Ag(111) surfaces suggest that the apparent universal behavior might be explained with a simple physical model. Therefore, we undertook a calculation of the *ns* resonance energy for Li through Cs, starting with the semiempirical potentials for the alkalis (pseudopotentials)[45] and the noble metal substrates (Chulkov potentials),[46] which accurately reproduce the electronic structures of the individual unperturbed systems, and their main mode of interaction through the Coulomb fields of the associated charges.

The uncoupled potentials of the combining surface and the adsorbate ion, and the derived effective potentials at the appropriate R_{ads} for Li/Cu(111) and Cs/Cu(111) are shown in Fig. 3. The uncoupled potentials align at their common reference level, E_{vac}.[3] The work function of Cu(111) (Φ =4.91 eV) (Ref. 47) and the atomic ionization potentials (I =5.39 to 3.89 eV for Li through Cs) are such that the *ns* states of alkalis straddle the E_F of the substrate.

Chemisorption modifies the electronic structures of the free adsorbates (atoms and molecules) through the chemical, image-charge, and (at higher coverages) adsorbate-adsorbate interactions. The image-charge interaction, which is dominant for alkali atoms interacting with metal surfaces,[18,19,23,48,49] arises from the many-body screening of an external charge by the conduction-band electrons in a metal. The screening response to an external charge can be described through the Coulomb field of its fictitious "image" charge, which has the opposite sign and is located at the position of the mirror image with respect to an image plane. The Chulkov potential, which accurately reproduces the surface structure and projected band gap of (111) surfaces of noble metals, locates the image plane at 2.1 and 2.2 a.u. above the top surface layer, respectively, of Cu(111) and Ag(111).[46] An *ns* electron of an alkali atom close to a metal surface experiences the attractive Coulomb potential of its own image $V_{IP}=-1/4z$ and the repulsive potential of the negatively charged image of the alkali-atom ionic core $V_{\Delta}=1/\sqrt{(R_{\mathrm{ads}}+z)^2+|\vec{\rho}|^2}$ (the electron distance z and adsorption height R_{ads} are measured along the z axis from the image plane, and $|\vec{\rho}|$ is the electron distance parallel to the surface from the adsorbate center).

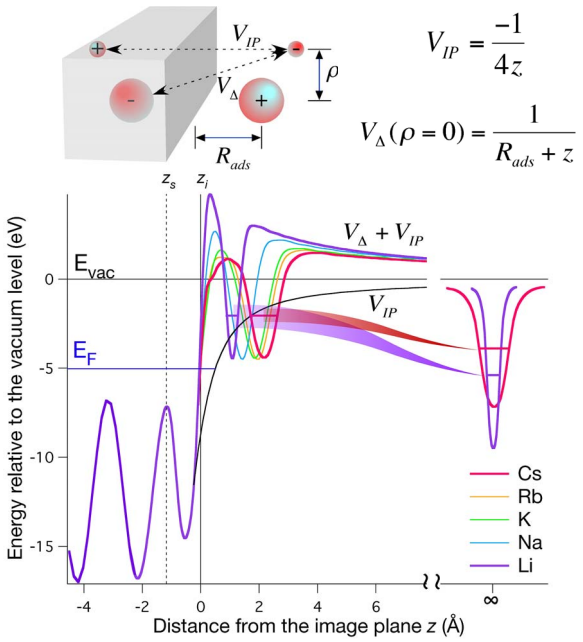

FIG. 3. (Color online) (top) The attractive image V_{IP} and repulsive ion core image-charge V_Δ interactions experienced by *ns* electrons of alkali atoms in front of a metal surface. (bottom) The effective one-electron potentials for Li through Cs atoms in front of Cu(111) surface. Potentials are plotted in units of Å along the z axis perpendicular to the surface and passing through the adsorbate center. The origin of z is the image plane. The clean surface image potential V_{IP} (black line) and representative free alkali atom pseudopotentials for Li and Cs are aligned to a common vacuum level E_{vac}. At the chemisorption height R_{ads}, the total effective potentials are constructed from the model potential of Chulkov *et al.* for Cu(111), which includes V_{IP} (Ref. 46), the Li pseudopotential- (Ref. 45), and the repulsive ion core image-charge potential V_Δ. The horizontal lines for Li and Cs represent the *ns* energy levels of free atoms and the antibonding resonance at R_{ads}. The curved lines connecting them convey the destabilization and broadening of *ns* states into the corresponding surface resonances when alkali atoms are transported to the surface.

According to the Gurney model for chemisorption, transporting a free alkali atom to R_{ads} lifts the energy of its *ns* electron through the Coulomb interaction with the conduction electrons of the substrate rendering it an unoccupied resonance in the electronic DOS.[18] Because the *ns* resonance is sharp (<0.2 eV) and its energy with respect to E_F is large (~ 3 eV), chemisorbed alkali atoms, according to this model, should be completely ionized at low coverage. The image-charge interactions lift the *ns* electron with respect to its free-atom energy by $\Delta E = \bar{V}_{IP} + \bar{V}_\Delta \approx +1/4R_{ads}$, where the approximate averaged potentials $\bar{V}_\Delta \approx +1/2R_{ads}$ and $\bar{V}_{IP} \approx -1/4R_{ads}$ assume the *ns* orbital to be centered on the ionic core ($z=R_{ads}, |\vec{\rho}|=0$). According to Figs. 1 and 2, independent of alkali-atom period, i.e., I or R_{ads}, the quasistationary state corresponding to the *ns* electron localized on the alkali adsorbate is bound, depending mainly on the substrate, by 1.8–2.0 eV with respect to E_{vac}. We note that semiempirical potentials similar to those presented in Fig. 3 have been used for a long time to address the scattering of alkali atoms or ions by metallic surfaces.[49] In that case, however, the potential and consequently the *ns* electron binding energy will evolve during the scattering trajectory according to the z dependence of the Coulomb interaction outlined above.

To rationalize the period-independent binding energy of AR on noble metals, we calculated the energies of the alkali-localized quasistationary states for a range of heights above Cu(111) and Ag(111) surfaces. The time-dependent Schrödinger equation was solved with a wave-packet propagation (WPP) method[48,50] for an electron evolving under the influence of the effective potential constructed by adding the core image-charge repulsion V_Δ to the semiempirical potentials of the free alkali atoms and the substrate (Fig. 3).[45,46] To account for change in the surface potential at finite alkali-atom coverages, which stabilizes AR, the contribution from the surface dipole field was also included.[43]

To compare the calculated AR energies in Fig. 4(a) with the experiment, the WPP results have to be taken at the correct R_{ads}. Because the experimental values of R_{ads} are available only for few systems and usually at a monolayer coverage,[7] we determined R_{ads} in the low coverage limit by plane-wave pseudopotential density functional theory (DFT) calculations of the optimized structures of Li through Cs on Cu(111) and Ag(111) surfaces. Using the generalized gradient approximation (GGA) to DFT with the Perdew-Becke-Ernzehof (PBE) functional,[51] we calculated the 2×2, 4×4, and 7×7 structures to extrapolate R_{ads} to the low coverage limit.[52–54] Decreasing the coverage from 2×2 to 7×7 increased R_{ads} by less than 6%. Because of inadequate treatment of electron correlation by the PBE functional, we found R_{ads} for Li to be $\sim 4\%$ shorter than the experimental one; as a remedy, we calculated R_{ads} for Li with a cluster calculation using the Becke three-parameter Lee-Yang-Parr functional.[52,53] Other alkali atoms exhibited much smaller functional dependence.

Figure 2(b) presents the calculated coverage-dependent AR binding energies for Li through Cs on Cu(111) and Ag(111). Despite their substantial periodic differences as free atoms, our theoretical approach predicts the common AR binding energies of -2.17 and -2.05 eV for the chemisorbed Li through Cs, respectively, on Cu(111) and Ag(111), which are in good agreement with all the experimental trends for these surfaces.

Based on the success in reproducing the electronic structure of chemisorbed alkali atoms with effective potentials, the period-independent binding energy of AR can be understood from simple arguments. Recalling that the *ns* electron localized around the ion experiences the repulsion ΔE due to the image-charge interactions, its binding energy E_b can be approximated by $E_b = \Delta E - I = 1/4R_{ads} - I$. Clearly, the common binding energy requires the period-dependent I to be compensated by ΔE to bring about the atom size or R_{ads}-independent difference. The compensation thus implies that for alkali atoms, there exists an anticorrelation between I and R_{ads}, which indeed is evident in the plot of I against the DFT values of R_{ads} for Li through Cs on Cu(111) and Ag(111) surfaces [Fig. 4(b)]. The anticorrelation is a consequence of screening of the Coulomb potential of the alkali-atom nucleus by its core electrons. Together the screened Coulomb potential and the Pauli exclusion establish how the

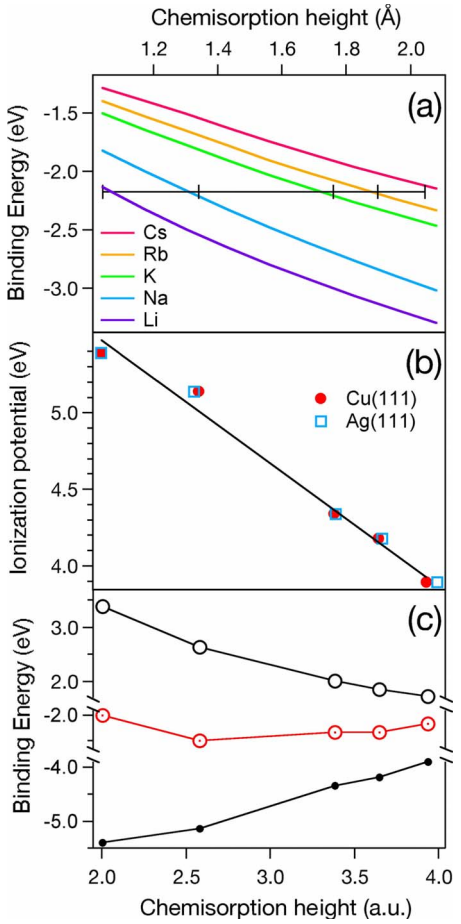

FIG. 4. (Color online) (a) The calculated AR energy as a function of the chemisorption height [R_{ads} is given in atomic units (bottom) and Å (top)] for Li through Cs on Cu(111). The horizontal line at −2.17 eV is the average alkali-atom AR binding energy from the WPP calculation taken at the R_{ads} from the DFT geometry optimization (indicated by the intersecting vertical lines). (b) The anticorrelation between R_{ads} for Li through Cs (left to right) and the free atom ionization potentials I for Cu(111) and Ag(111). (c) The electron binding energy of the free alkali ions ($-I$; solid circles) and the total level shift $\Delta E=\bar{V}_{\Delta}+\bar{V}_{IP}=1/4R_{\mathrm{ads}}$ (open circles) together define the AR binding energy $E_b=\Delta E-I$ at R_{ads} (bulls eye) for Li through Cs on Cu(111).

ionic alkali core interacts with its *ns* valence electron, as well as the conduction electrons of the substrate. The binding energy I of *ns* valence electron of a free alkali atom is related through Coulomb interaction and Pauli exclusion to its chemisorption distance R_{ads}.

Figure 4(c) shows explicitly the component repulsive $\Delta E=1/4R_{\mathrm{ads}}$ and attractive $-I$ interactions given by R_{ads} from the DFT chemisorption structure and the atomic ionization potentials. The two interactions combine to give the binding energy E_b of *ns* valence electrons at R_{ads} on Cu(111). The electron binding energy of the free alkali atoms ($-I$; circles) and the image-charge repulsion (ΔE; open circles) grow in magnitude with the opposite sign as R_{ads} decreases. In their sum $E_b=\Delta E-I$ (bull's eye), however, their periodic trends are compensated to give an average AR binding energy of −2.26 eV, in agreement with the more elaborate WPP model.

Finally we note that the success of our model for the alkali atom/noble metal interaction in predicting the unoccupied electronic structure of the chemisorption interface supports the long held view by Langmuir, Gurney, and others that the interaction is mainly of the ionic nature.[17,18] This view does not preclude that covalent interactions may play a minor, but increasingly important role, for smaller alkali atoms and transition-metal surfaces.[13,22]

V. CONCLUSIONS

Our simple model, which accounts for only the Coulomb interaction and the Pauli exclusion experienced by the *ns* valence electron of the free and chemisorbed alkali atoms, and excludes the covalent interactions where valence electrons occupy the orbitals shared between the adsorbate and the substrate, is in excellent agreement with both the full three-dimensional WPP calculation and experiments. It explains the alkali-atom period-independent electronic structure of the chemisorption interface in terms of purely ionic interactions. Thus, given only the free-molecule electron binding energy and R_{ads}, for an atom or a molecule with a well-defined charge configuration in both its highest occupied molecular orbitals (HOMO) and the lowest unoccupied molecular orbitals (LUMO), our theoretical model predicts accurately the energy of the quasistationary state at the metal-adsorbate interface.

Our results confirm the crucial role of the image-charge effects for defining the positions HOMO and LUMO of a broad class of adsorbed molecules on metals. While the important role of the interfacial dipole potential has been widely recognized,[3,5,55] the dominant V_{IP} contribution is frequently neglected. For example, it is absent from DFT calculations. The HOMO, and more generally the ionization level, of adsorbates on metals are lifted by $\Delta E=1/4R_{\mathrm{ads}}$ due to the interaction with the image charge. For the alkalis this effect exactly compensates the variation of the atomic I and produces a period-independent binding energy of AR. The electronic image potential stabilizes the LUMO, or affinity level, by a similar amount of $-1/4R_{\mathrm{ads}}$, leading to a HOMO-LUMO gap reduction of $1/2R_{\mathrm{ads}}$. To reproduce this effect from first principles requires theoretical approaches beyond the DFT level of theory, as shown by recent calculations for benzene physisorption on graphite, in which many-body effects were included using perturbation theory.[15] Instead, the simple modeling used here reproduces these shifts well as far as the electronic states are localized on the adsorbates rather than shared in a covalent bond. Thus, we expect our model to provide valuable insight into the design of metal/molecule interfaces with desired electronic properties.

ACKNOWLEDGMENTS

H.P. and J.Z. acknowledge J. W. Gadzuk for insightful discussions. This work was supported by the U.S. Department of Energy Grant No. DE-FG02-03ER15434. Some calculations were performed in the Environmental Molecular

Sciences Laboratory, a user facility sponsored by the DOE Office of Biological and Environmental Research. N.P. thanks the Alexander von Humboldt Foundation for support. H.P. thanks Ikerbasque for the support of his stay at DIPC. The San Sebastián group acknowledges support by the Spanish MEC grant, the European FP6-NoE grant "Nanoquanta," the UPV/EHU and the projects "NANOMATERIALES" and "NANOTRON" of the Basque Government and the Diputación de Guipúzcoa.

*petek@pitt.edu

[1] N. F. Mott, Proc. Cambridge Philos. Soc. **34**, 568 (1938).
[2] W. Schottky, Z. Phys. **118**, 539 (1942).
[3] H. Ishii, K. Sugiyama, E. Ito, and K. Seki, Adv. Mater. (Weinheim, Ger.) **11**, 605 (1999).
[4] X. Y. Zhu, Surf. Sci. Rep. **56**, 1 (2004).
[5] D. Cahen, A. Kahn, and E. Umbach, Mater. Today **8**, 32 (2005).
[6] F. S. Tautz, Prog. Surf. Sci. **82**, 479 (2007).
[7] R. D. Diehl and R. McGrath, J. Phys. C **9**, 951 (1997).
[8] M. Bauer, S. Pawlik, and M. Aeschlimann, Phys. Rev. B **55**, 10040 (1997).
[9] H. Petek, M. J. Weida, H. Nagano, and S. Ogawa, Science **288**, 1402 (2000).
[10] H. Petek, H. Nagano, M. J. Weida, and S. Ogawa, J. Phys. Chem. B **105**, 6767 (2001).
[11] A. G. Borisov, J. P. Gauyacq, A. K. Kazansky, E. V. Chulkov, V. M. Silkin, and P. M. Echenique, Phys. Rev. Lett. **86**, 488 (2001).
[12] A. G. Borisov, J. P. Gauyacq, E. V. Chulkov, V. M. Silkin, and P. M. Echenique, Phys. Rev. B **65**, 235434 (2002).
[13] K. Niedfeldt, P. Nordlander, and E. A. Carter, Phys. Rev. B **74**, 115109 (2006).
[14] T. Klüner, N. Govind, Y. A. Wang, and E. A. Carter, Phys. Rev. Lett. **86**, 5954 (2001).
[15] J. B. Neaton, M. S. Hybertsen, and S. G. Louie, Phys. Rev. Lett. **97**, 216405 (2006).
[16] H. P. Bonzel, A. M. Bradshaw, and G. Ertl, *Physics and Chemistry of Alkali Metal Adsorption* (Elsevier, Amsterdam, 1989).
[17] I. Langmuir, Phys. Rev. **43**, 224 (1933).
[18] R. W. Gurney, Phys. Rev. **47**, 479 (1935).
[19] J. W. Gadzuk, Surf. Sci. **6**, 133 (1967).
[20] N. D. Lang and A. R. Williams, Phys. Rev. B **18**, 616 (1978).
[21] J. P. Muscat and D. M. Newns, Prog. Surf. Sci. **9**, 1 (1978).
[22] H. Ishida, Phys. Rev. B **38**, 8006 (1988).
[23] P. Nordlander and J. C. Tully, Phys. Rev. B **42**, 5564 (1990).
[24] B. Woratschek, W. Sesselmann, J. Küppers, G. Ertl, and H. Haberland, Phys. Rev. Lett. **55**, 1231 (1985).
[25] G. K. Wertheim, D. M. Riffe, and P. H. Citrin, Phys. Rev. B **49**, 4834 (1994).
[26] H. Ishida, Phys. Rev. B **39**, 5492 (1989).
[27] C. Stampfl, J. Neugebauer, and M. Scheffler, Surf. Sci. **307-309**, 8 (1994).
[28] D. A. Arena, F. G. Curti, and R. A. Bartynski, Phys. Rev. B **56**, 15404 (1997).
[29] N. Fischer, S. Schuppler, R. Fischer, Th. Fauster, and W. Steinmann, Phys. Rev. B **47**, 4705 (1993).
[30] N. Fischer, S. Schuppler, Th. Fauster, and W. Steinmann, Surf. Sci. **314**, 89 (1994).
[31] M. Bauer, S. Pawlik, and M. Aeschlimann, Phys. Rev. B **60**, 5016 (1999).
[32] S. Ogawa, H. Nagano, and H. Petek, Phys. Rev. Lett. **82**, 1931 (1999).
[33] H. Petek, M. J. Weida, H. Nagano, and S. Ogawa, Surf. Sci. **451**, 22 (2000).
[34] H. Petek and S. Ogawa, Annu. Rev. Phys. Chem. **53**, 507 (2002).
[35] J. P. Gauyacq, A. G. Borisov, and M. Bauer, Prog. Surf. Sci. **82**, 244 (2007).
[36] K. Onda, B. Li, and H. Petek, Phys. Rev. B **70**, 045415 (2004).
[37] K. Onda, B. Li, J. Zhao, K. D. Jordan, J. Yang, and H. Petek, Science **308**, 1154 (2005).
[38] H. Petek and S. Ogawa, Prog. Surf. Sci. **56**, 239 (1997).
[39] S. A. Lindgren and L. Walldén, Phys. Rev. B **45**, 6345 (1992).
[40] N. Pontius, V. Sametoglu, and H. Petek, Phys. Rev. B **72**, 115105 (2005).
[41] M. Weinelt, J. Phys.: Condens. Matter **14**, R1099 (2002).
[42] H. Petek, H. Nagano, M. J. Weida, and S. Ogawa, Chem. Phys. **251**, 71 (2000).
[43] A. G. Borisov, A. K. Kazansky, and J. P. Gauyacq, Surf. Sci. **430**, 165 (1999).
[44] H. Petek, H. Nagano, M. J. Weida, and S. Ogawa, J. Phys. Chem. A **104**, 10234 (2000).
[45] J. N. Bardsley, Case Stud. At. Phys. **4**, 299 (1974).
[46] E. V. Chulkov, V. M. Silkin, and P. M. Echenique, Surf. Sci. **437**, 330 (1999).
[47] H. Kawano, Prog. Surf. Sci. **83**, 1 (2008).
[48] A. G. Borisov, A. K. Kazansky, and J. P. Gauyacq, Phys. Rev. B **59**, 10935 (1999).
[49] H. Winter, Phys. Rep. **367**, 387 (2002).
[50] E. V. Chulkov, A. G. Borisov, J. P. Gauyacq, D. Sanchez-Portal, V. M. Silkin, V. P. Zhukov, and P. M. Echenique, Chem. Rev. (Washington, D.C.) **106**, 4160 (2006).
[51] J. P. Perdew, K. Burke, and M. Ernzerhof, Phys. Rev. Lett. **77**, 3865 (1996).
[52] A. D. Becke, J. Chem. Phys. **98**, 5648 (1993).
[53] C. Lee, W. Yang, and R. G. Parr, Phys. Rev. B **37**, 785 (1988).
[54] G. S.-M. Tong and A. S. C. Cheung, J. Phys. Chem. A **106**, 11637 (2002).
[55] G. Witte, S. Lukas, P. S. Bagus, and C. Wöll, Appl. Phys. Lett. **87**, 263502 (2005).